

Modeling polymer melt-flow instabilities

J. Molenaar

*Faculty of Mathematics and Computing Science, Eindhoven University
of Technology, The Netherlands*

R. J. Koopmans^{a)}

*Dow Benelux N. V., Polyolefins & Elastomers R&D, 4530 AA Terneuzen,
The Netherlands*

(Received 18 February, 1993; accepted 18 September, 1993)

Synopsis

The long-standing problem of polymer melt-flow instabilities is looked upon from a new and quite general mathematical viewpoint. A single mathematical model is developed allowing the macroscopic description of measurable state variables characterizing the different melt-flow instability regimes. Based on the theory of relaxation oscillations, a set of two coupled first-order ordinary differential equations, relating state variables—pressure and flow rate—provides sufficient degrees of freedom to describe all the relevant flow regimes in shear flow. By means of this model, the appearance of extrudate distortions can be expressed in terms of pressure and output fluctuations without the need to invoke a microscopic theory. The analysis contains the potential for practical melt-flow instability predictions.

I. INTRODUCTION

For more than 30 years it has been known that a polymer melt passing through a die may exhibit flow instabilities [see, e.g., Tordella (1956)]. These phenomena, visually observed as distortions of the extrudate, are a serious problem in the polymer processing industry, limiting the production rates and the technological opportunities of the resins. In recent years much attention has been devoted to the subject. A comprehensive literature elaborating the different points of view on this issue can be found in some excellent review papers by Petrie and Denn (1976), Denn (1990), Larson (1992), and Denn (1992).

For polyolefin resins [i.e., high-density polyethylene (HDPE) and linear low-density polyethylene (LLDPE), which are mostly studied in this context] five distinct flow regimes can be identified [e.g., Becker *et al.* (1991) and Sornberger *et al.* (1987)]. Figure 1 shows a diagram for shear flow in a capillary die of pressure versus output representing the five regimes. Regime I corresponds to a smooth and often transparent extrudate. Here ordinary viscoelastic flow occurs and the pressure, as a function of time, is constant in steady shear. Regime II reflects an opaque extrudate with varying levels of surface roughness known as “sharkskin.” In steady shear and similar to

^{a)}To whom all correspondence should be addressed.

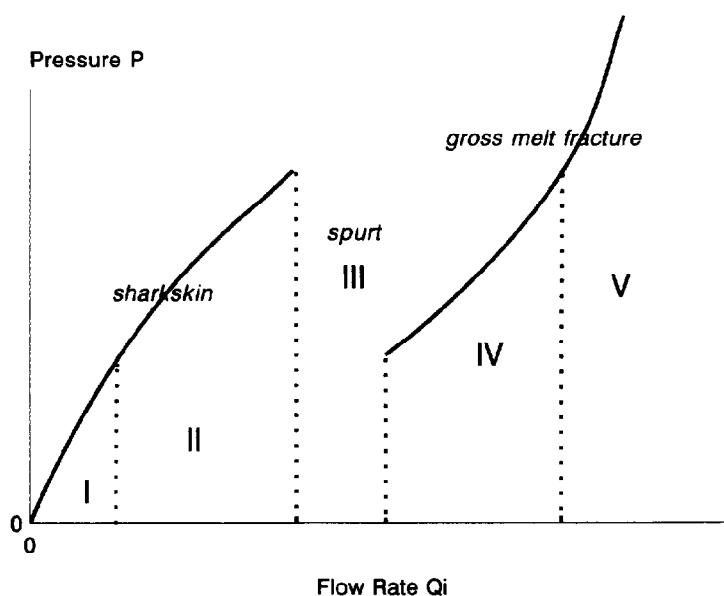


FIG. 1. A graphical representation of a typical relation between pressure in the barrel and the flow rate of the extrudate for a capillary rheometer experiment. The four different flow regimes identified as I, II, III are associated with the occurrence of different types of extrudate distortions, i.e., steady state, "sharkskin," "spurt," and melt fracture, respectively. Regimes IV and V are associated with the occurrence of various types of "gross" melt fracture.

regime I, the pressure remains constant as function of time. Even though, in this regime, the extrudate shows clearly "sharkskin," Beaufils *et al.* (1989) pointed out that perfectly stable flow birefringence patterns are observed, which are typical for ordinary viscoelastic flow and which correspond to a constant pressure measurement as a function of time. For regime III the extrudate emerges from the capillary in bursts and appears to have alternate smooth and rough surfaces. This regime is often referred to as the "stick-slip" or "spurt" regime. The pressure signal shows a "sawtooth" pattern as a function of time. In regimes IV and V the emerging melt can manifest itself as a smooth, spiraling, or strongly distorted extrudate known as "gross" melt fracture. The pressure signal, as a function of time, is again constant, similar to regimes I and II. In regime IV and for certain polymers, it is possible to observe an initial pressure "overshoot," followed by a constant pressure signal as function of time [see, e.g., Uhland (1979), who studied HDPE]. Pictures of these distorted extrudates can be found in papers by, for example, Bergem (1976), Lin (1985), El Kissi and Piau (1990), and Hatzikiriakos (1992).

In the present paper, the approach is to pursue the development of a single, mathematical model which will allow the description of measurable, macroscopic variables associated with all the observed melt-flow instability flow regimes. The formulation of such a basic model is intended to assist in the development of a more unified physical understanding of the phenomena, without referring to any specific microscopic model known to date. The currently proposed model may be considered to be an extension of the work of Weill (1980a).

On observing the "sawtooth" pressure signal as a function of time in the "spurt" regime III, when performing a capillary die experiment, it can be noticed that it strongly resembles a relaxation oscillation. The latter is well understood from a mathematical point of view. Relaxation oscillations can be described only in terms of second-order instead of first-order differential equations as used by Weill's model (1980b). The model accepts the nonisotropic, inhomogeneous nature of the polymer under certain boundary conditions.

II. A GENERAL MODELING APPROACH TO MELT-FLOW INSTABILITIES

A relaxation oscillation is a cyclic phenomenon during which potential energy is successively stored and relaxed. Relaxation oscillations were observed and studied for the first time by Van der Pol (1926) in a triode circuit. Such a system exhibits self-sustained oscillations with an amplitude independent of the starting conditions. For certain values of the system parameters, the oscillation is almost sinusoidal, while in a different range the oscillation shows abrupt changes due to the nonlinear behavior of the damping function. These self-excited oscillations are an important class of nonlinear phenomena and can occur in systems that have no periodic inputs or periodic forces [e.g., Moon (1987)]. In each case there is a steady source of energy and a source of dissipation or a nonlinear restraining mechanism. The mathematical background of the relaxation oscillations is described in detail by Grasman (1987). Essential ingredients are a second-order differential equation, or equivalently, two coupled first-order differential equations, one of which has a dimensionless parameter ϵ which is very small ($\epsilon \ll 1$). This system of two coupled first-order differential equations can be represented in a general form as:

$$\frac{dy}{dt} = -x, \quad (1)$$

$$\epsilon \frac{dx}{dt} = y - F(x). \quad (2)$$

Lienard (1928) studied systems of this type, with $F(x)$ such that the system has a relaxation oscillation. The Van der Pol equation with $F(x) = 1/3x^3 - x$ belongs to this class.

The experiment to be modeled is presented in Fig. 2. It contains a capillary rheometer for which the following parameters can be defined: v_p is the constant plunger speed; A is the cross-sectional area of the barrel and the plunger; Q_i is the constant inlet flow rate, Av_p ; $Q_e(t)$ is the extrudate flow rate; $P(t)$ is the pressure in the barrel; $\rho(t)$ is the melt density at pressure $P(t)$ and constant temperature; $h(t)$ is the distance from the plunger to the capillary; and χ is the melt compressibility, assumed to be uniform and constant.

The first differential equation of the set of two expresses the conservation of mass:

$$\frac{d}{dt} (Ah\rho) + \rho Q_e = 0. \quad (3)$$

The melt compressibility is related to $\rho(t)$ and $P(t)$, satisfying the equation

$$\frac{1}{\rho} \dot{\rho} = \chi \dot{P}, \quad (4)$$

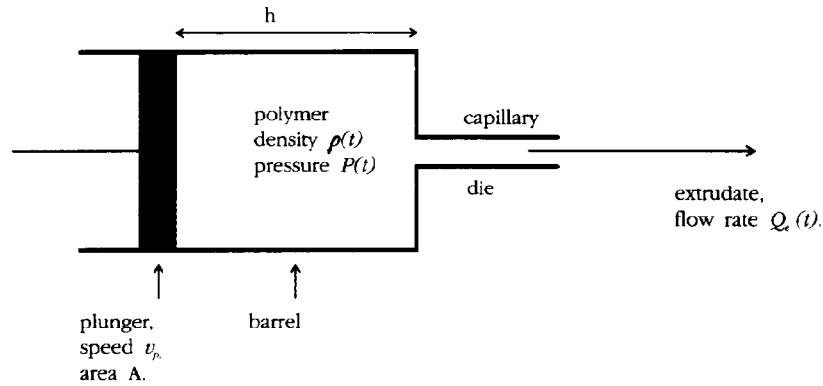


FIG. 2. A schematic representation of a capillary rheometer experiment used to model capillary polymer melt-flow instabilities in shear.

with

$$\dot{\rho} \equiv \frac{d}{dt} \rho, \quad \dot{P} \equiv \frac{d}{dt} P. \quad (5)$$

The barrel height is related to the plunger speed by

$$\frac{d}{dt} h \equiv \dot{h} = -v_p. \quad (6)$$

Using Eqs. (4) and (6), Eq. (3) can be rewritten as

$$\dot{P} = \frac{1}{C} (Q_i - Q_e), \quad (7)$$

with C being defined as

$$C \equiv A\chi h. \quad (8)$$

This product of barrel volume Ah and melt compressibility χ can be interpreted as the capacity of the system (\equiv melt) to store potential (\equiv internal) energy. Because the volume of the capillary is much smaller than the barrel volume, the capacity of the capillary can be ignored. The interpretation of Eq. (7) is clear: if $Q_i - Q_e > 0$ (< 0) the total mass in the barrel will increase (decrease), causing a positive (negative) change in the pressure. Equation (7) is a reflection of Eq. (1) and the first differential equation of the system. It expresses the dynamics of mass buildup in terms of pressure and density changes.

Now, the equivalent of Eq. (2) has to be derived. As Eq. (7) relates the *change* of pressure with time to a change in the total mass of the barrel, there must exist a functional relationship between the pressure and the flow rate:

$$P(t) = F[\Delta Q(t)] = \int_{t_0}^t \frac{1}{C(t')} [Q_i - Q_e(t')] dt', \quad (9)$$

with $\Delta Q \equiv Q_e(t) - Q_i$.

The function F is a general expression which can be obtained from one or more constitutive equations describing the polymer and its boundary condition. Now, the second differential equation can be derived by assuming that, if the pressure calculated from Eq. (7) deviates from F , this is corrected by some mechanism in the material. Phenomenologically, this mechanism can be described by

$$\frac{d}{dt}[Q_e(t) - Q_i] = \frac{d}{dt} Q_e \equiv \dot{Q}_e = \frac{1}{K}[P - F(\Delta Q)]. \quad (10)$$

The proportionality factor K^{-1} measures the ability of the melt to adjust the pressure via adjustment of the flow rate. The parameter K is assumed to be constant in time, but it may depend on the geometry and the material under consideration.

The basic model describing the polymer flow consists of the coupled equations (7) and (10). For given F , Q_i , C , K , and initial conditions $Q_e(0)$ and $P(0)$, this system of ordinary differential equations can be integrated in time, resulting in the solution $[Q_e(t), P(t)]$, $t > 0$.

To analyze the model qualitatively it is necessary to put it into a dimensionless form. For that purpose it is useful to know typical values of the parameters:

$$Q_i \approx 10^{-8} \text{ m}^3/\text{s},$$

$$P \approx 10^7 \text{ Pa},$$

$$\chi \approx 10^{-9} \text{ Pa}^{-1},$$

$$A \approx 10^{-4} \text{ m}^2,$$

$$h \approx 10^{-1} \text{ m},$$

$$v_p \approx 10^{-4} \text{ m/s}.$$

From Eq. (8) one sees that C is time dependent through h . Using Eq. (6) and the typical values above, an estimate for the relative change in C is found from

$$\frac{1}{C} \frac{d}{dt} C = -\frac{v_p}{h} \approx 10^{-3} \text{ s}^{-1}. \quad (11)$$

This relative change in C , which is proportional to the (constant) plunger speed, is much smaller than the typical frequency of sharkskin and spurt events, reported as 50 and 0.5 Hz, respectively, by Weill (1980b). By fixing the value of h , C can be reliably considered as a constant.

In the dimensional analysis, a characteristic pressure value P_0 is needed. For typical polymer melt applications, a natural choice is $P_0 = 10^7$ Pa. With this choice the dimensionless time t^* is given by

$$t^* \equiv \left(\frac{CP_0}{Q_i} \right)^{-1} t. \quad (12)$$

The flow rates are naturally scaled with Q_i :

$$Q_e^*(t^*) \equiv \frac{Q_e(t)}{Q_i}, \quad (13)$$

$$\Delta Q^*(t^*) \equiv \frac{\Delta Q(t)}{Q_i}, \quad (14)$$

$$Q_i^* \equiv 1, \quad (15)$$

and the pressures with P_0 :

$$P^*(t^*) \equiv \frac{P(t)}{P_0}, \quad (16)$$

$$F^*(\Delta Q^*) \equiv \frac{F(\Delta Q)}{P_0}. \quad (17)$$

Substitution of the dimensionless quantities into model equations (10) and (7) leads to

$$\frac{d}{dt^*} \Delta Q^* = \frac{1}{\epsilon} [P^* - F^*(\Delta Q^*)], \quad (18)$$

$$\frac{d}{dt^*} P^* = -\Delta Q^*. \quad (19)$$

This dimensionless model contains only one parameter ϵ , defined by

$$\epsilon \equiv \frac{KQ_i^2}{CP_0^2}. \quad (20)$$

This model is a reflection of Eqs. (2) and (1), respectively. In Sec. III, it will be shown that the model can conveniently describe all the observed melt-flow instabilities as long as $\epsilon \ll 1$. Using the typical parameter values specified above, this condition is satisfied if $K \ll 10^{16} \text{ kg/m}^4$ (or $\text{Pa s}^2/\text{m}^3$, which suggests the dimensions of a normal stress coefficient per unit volume). Under this condition the solutions of the model are independent of the precise value of this parameter. The parameter K has been introduced heuristically. Throughout the paper it is taken for granted that in the above it is true that $\epsilon \ll 1$. The behavior of the solutions of the model is best understood using the phase plane spanned by the ΔQ^* and P^* axes.

III. PHASE PLANE ANALYSIS

The phase plane is the set of possible state vectors, the components of a state vector being the basic variables of the system under consideration. In this case the phase plane is defined by ΔQ^* and P^* . Using the phase plane technique, the dependency of the solutions of the set of coupled first-order differential equations on the shape of the F curve can be demonstrated. Before dealing with specific F curves, some general features of the model will be evaluated.

Because $\epsilon \ll 1$, it can be seen from Eq. (18) that ΔQ^* will change dramatically as soon as P^* deviates from F^* . So, wherever one starts in the phase plane (except for the origin), the solution will immediately jump to the F^* curve along a nearly horizontal line. Thereafter, it will tend to stay on the curve $P^* = F^*$.

Equations (18) and (19) have one or more equilibrium points (EP) (\equiv singular points) given by $\Delta Q^* = 0, P^* = F^*(0)$. These are obtained by setting the right-hand sides of the equations equal to zero. Note that F^* may be multivalued in 0. At an EP,

$Q_e = Q_i$ and the pressure is thus constant. The (in)stability of an EP determines the character of the solution in its vicinity. Following a well-known stability theory [see, e.g., Willems (1970)], the stability properties of an EP can be found by linearizing the right-hand sides of Eqs. (18) and (19) and looking at the eigenvalues of the resulting Jacobi matrix. Omitting the mathematical details, the following results can be reported. If the derivative of F^* in an EP is positive, the EP is a positive attractor, i.e., solutions starting in the proximity of the EP are attracted towards the EP and stay there. If the derivative is negative, the EP is a negative attractor, i.e., it repulses solutions. If the derivative is vanishing, the EP is a center and the solutions tend to circle around it without approaching it. From these insights it is possible to discern four regimes for the F^* curve. It is important to recall that the function F^* is a general dimensionless expression associated with a constitutive equation. It is a mathematical formalism to describe the macroscopic melt-flow behavior. The physical meaning of F^* is defined by the physical interpretation of the constitutive equation and in this context it is independent of any microscopic theory.

Based on the mathematical stability analysis, it is possible to consider four functional forms for F^* as represented in Fig. 3. It should be clear, that the functional form of F^* depends on the material (\equiv polymer), i.e., F^* can but must not necessarily be nonmonotonic as shown in Figs. 3(c) and 3(d). However, a nonmonotonic constitutive equation or equivalently a nonmonotonic F^* curve can be associated with all commercially available polyolefin polymers. For such a case, depending on the boundary conditions of the flow, i.e., die geometry and flow rate, the F^* curve has at least three different regimes for which the nature of the EP corresponds to the situations depicted in Figs. 3(a), 3(b), and 3(c). This implies that for a fixed die geometry and a given polymer with which a nonmonotonic F^* can be associated, an increasing flow rate (i.e., changing boundary conditions) will consecutively define the three (four in the most general case) specific shapes of F^* . In turn, these can be associated with a different flow instability phenomenon that should be observable in terms of the state variables pressure and flow rate. The four possible cases are as follows:

(i) In Fig. 3(a), a strictly monotonically increasing F^* curve is drawn in the $(\Delta Q^*, P^*)$ plane. The equilibrium point $[0, F^*(0)]$, indicated by EP, is a positive attractor. In the experimental practice the system will start at $t = 0$ in point A in Fig. 3(a). The pressure and extrudate flow rate are still vanishing and the plunger is just set in motion, so $\Delta Q^* = -Q_i$. For $t > 0$, the solution will follow the dashed curve in Fig. 3(a) along the F^* curve and end up at the EP. The corresponding curves of $Q_e(t)$ and $P(t)$ are also shown in Fig. 3(a).

(ii) In Fig. 3(b), the F^* curve has a plateau around $\Delta Q^* = 0$. The EP is now a center, because F^* has a vanishing derivative. Starting at A, the solution will initially follow F^* towards EP. In the vicinity of the EP it will start circling around it. The $Q_e(t)$ and $P(t)$ curves are also shown in Fig. 3(b). The variations in Q_e will be relatively larger than those in P , with the ratio depending on the length of the plateau in the F^* curve.

(iii) In Fig. 3(c), the derivative of F^* at EP is negative, so the EP is unstable and will repulse solutions. After the transient AB, the solution will follow the periodical path BCDEB. This can be understood as follows. Starting from A, the solution moves along F^* towards C. Because of Eq. (17), the pressure P^* must become larger there. Therefore, the solution leaves the F^* curve and jumps from C to D. Next, the solution follows the F^* curve again towards E and there a second jump from E to B takes place, completing one relaxation oscillation. It should be noted that the solution spends hardly any time (in the order of ϵ) between C and D and between E and B. The

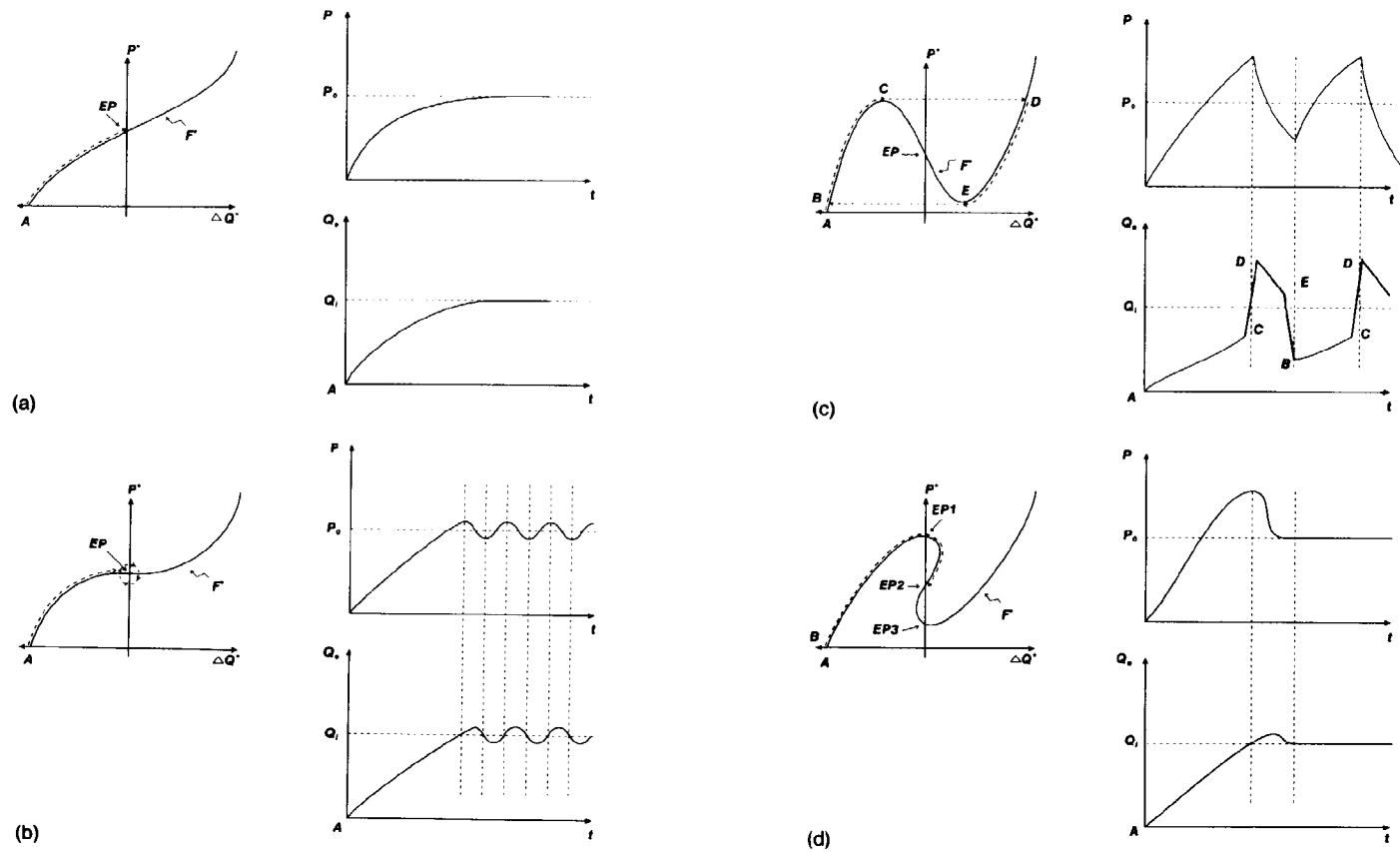


FIG. 3. A schematic phase plane representation of ΔQ^* vs P^* for four possible functional forms of F^* [(a)-(d)] and the associated solution of the set of two coupled first-order differential equations comprising the model for $P(t)$ and $Q_e(t)$.

$Q_e(t)$ and $P(t)$ curves are also shown in Fig. 3(c). Note that the extrema in Q_e and P are just out of phase.

(iv) In Fig. 3(d), F^* is multivalued and there are three equilibrium points EP1,2,3. EP2 is a positive attractor and EP1 and EP3 are centers. Starting at A, the solution will move along F^* to EP1. Because EP1 is not attracting, the solution will pass it and follow the F^* curve until it reaches EP2, where it remains. The $Q_e(t)$ and $P(t)$ curves are also shown in Fig. 3(d). Both curves approach equilibrium after showing an overshoot.

It is clear that cases (i)–(iv) discussed above are sufficient to describe mathematically the four flow regimes, shown in Fig. 1, and consequently the associated pressure and flow-rate fluctuations. Now, some plausible considerations can be made to relate these mathematical results to the various physical observations in capillary polymer melt flow.

In regime I of Fig. 1, the system is in the steady-state mode. Each point in this regime is experimentally defined by a constant pressure and Q_e . For a capillary experiment it is known that this constant pressure is only gradually reached after a certain time. For $Q_e(t)$ a similar result occurs [see Fig. 3(a)]. At higher plunger speeds the time to reach the steady state will become shorter. This regime is a clear illustration of case (i).

In regime II, experiments show the presence of surface defects ("sharkskin"). The intensity of the surface defects increases with increasing plunger speed. The mathematical condition corresponding to this regime could be associated with case (ii). When the F^* curve has a plateau, sharkskin occurs. For nearly all polymers, being polydisperse, the F^* curve or equivalently the constitutive equation is not strictly monotonically increasing. The presence of a plateau implies that for a given shear stress, the shear rate can have more than one value. The condition of two shear rates for one pressure is discussed by Hunter and Slemrod (1983) and McLeisch and Ball (1986), and is a sufficient condition for a spatial segregation of flow to occur. The existence of two layers, a high shear rate one at the die wall and a lower shear rate one at the core, can be considered as a "pseudo" equilibrium condition of the flow. The analogy with a phase diagram in which two phases of the same material can coexist, e.g., solid (ice) and liquid water, may be appropriate. Waddon and Keller (1992) showed in pressure-temperature diagrams of polyethylene resins the possibility for a "strain-induced formation of a mobile mesophase." Such a situation should not give rise to any observable flow instability in the die as the mathematical model describing this regime has (only) two real solutions for shear rate. However, when the material exits the die, the boundary conditions change, and the circumstances maintaining this "pseudo" equilibrium condition will vanish. The existence of a differential strain in the material in the die can manifest itself only at the die exit by a differential recovery of the material. As the relaxation of the material will be different at the extrudate surface than at the core, a surface defect occurs. The high-frequency, small-amplitude $P(t)$ and $Q_e(t)$ response as shown in Fig. 3(b) will only be observable when the EP is a true center and the material does not allow an adjustment of the pressure via a readjustment of the flow rate.

In this context, it should be worthwhile to define experimentally the shear rate at which the second branch of the Fig. 1 curve starts as it should determine the critical stress for the onset of "sharkskin." Accordingly, the definition of a universal critical shear stress value for the onset of surface defects, as is common in literature, is only of relative use as it depends on the nature of the constitutive equation and therefore the associated polymer composition.

In regime III, periodical, spurting flow instabilities occur with dominant oscillations in pressure and $Q_e(t)$. This is typical for a relaxation oscillation, i.e., a self-excited oscillation caused by a steady (nonperiodic) source of energy, imposed on a material which can dissipate energy. The experimental observations of $P(t)$ can be described by the relaxation oscillation as defined in case (iii). As in case (ii), the shape of the pressure and $Q_e(t)$ function will depend on the composition of the material and will eventually be defined by the function F^* . No equilibrium state can be found in contrast to regime II. The amplitude and frequency of the relaxation oscillation will depend on the die geometry, the flow rate, and the nature of the polymer. The shape of the F^* curve will define the range of the "spurt" defect regime to the extent that it is defined by the shear rate interval starting at the end of regime II [point C in Fig. 3(c)] and the start of a high shear rate "steady-state" pressure measurement, i.e., the second branch [point E in Fig. 3(c)]. If the nonmonotonic F^* curve has the shape of Fig. 3(d), the pressure signal is generally characterized by an overshoot, followed by a period wherein the pressure remains constant. This situation corresponds to the mathematical formalism of case (iv).

In regime IV, the flow seems to have reached a second stable mode but different from the one in regime I. As in regime II, two values of the shear rate can be associated with each stress value. In this situation, a spatial segregation could again occur and possibly with the "high" shear rate phase in the center of the material and the "low" shear rate phase at the die. For certain materials this could be reflected in an apparent smooth surface.

The shape of the extrudate may become distorted as die entry effects can be important, e.g., vortex formation in the barrel before the die entrance can give the extrudate a "cork-screw" appearance [e.g., Bergem (1976)]. The extrudate can have different degrees of distortion depending on the geometry of barrel, the die, and the material under study.

According to the present reasoning, regime V can be defined as starting at pressures or flow rates above point D as defined in Fig. 3(c). Again, an ordinary steady-state mode is reached, describable in terms of case (i). However, inlet effects may become the dominating factors for defining the final distortion of the extrudate.

IV. CONCLUSIONS

Although the current model is quite simple, it allows one to describe all the observable macroscopic flow instabilities of polymer melts in a consistent way. It is also clear that the exact functional form of F^* , which contains material parameters, being equivalent to a constitutive equation, will determine the qualitative and quantitative features of a polymer flow. The general model of two coupled first-order differential equation takes into account the effect of die geometry and defines the compressibility of the material as an essential parameter to describe polymer melt-flow instabilities in terms of the macroscopic state variables, pressure and flow rate.

ACKNOWLEDGMENTS

R. J. K. acknowledges the stimulating discussions with D. Porter of DOW Benelux N. V., and with J. F. Agassant, B. Vergnes, and V. Durand of CEMEF. The critical comments offered by J. Dealy are much appreciated.

References

- Beaufils, P., B. Vergnes, and J. F. Agassant, "Characterization of the sharkskin defect and its development with the flow conditions," *Int. Polym. Proc.* **VI-2**, 78-84 (1989).
- Becker, J., P. Bengtsson, C. Klason, J. Kubat, and P. Saha, "Pressure oscillations during capillary extrusion of high density polyethylene," *Int. Polym. Proc.* **VI-4**, 318-325 (1991).
- Bergem, N., "Visualization studies of polymer melt flow anomalies in extrusion," *Proceedings of the VIIIth International Congress on Rheology, Göteborg, Sweden, 1976*, pp. 50-54.
- Denn, M. M., "Issues in viscoelastic fluid mechanics," *Ann. Rev. Fluid. Mech.* **22**, 13-34 (1990).
- Denn, M. M., "Surface induced effects in polymer melt flow," *Proceedings of the XIth International Congress on Rheology, Brussels, Belgium, 1992*, pp. 45-49.
- El Kissi, N. and J. M. Piau, "The different capillary flow regimes of entangled polydimethylsiloxane polymers: Macroscopic slip at the wall, hysteresis and cork flow," *J. Non-Newt. Fluid Mech.* **37**, 55-94 (1990).
- Grasman J., *Asymptotic Methods for Relaxation Oscillations and Applications*, Vol. 63 of *Applied Mathematical Sciences* (Springer, New York, 1987).
- Hatzikiriakos, S. G. and J. M. Dealy, "Wall slip of molten high density polyethylene. II. Capillary rheometer studies," *J. Rheol.* **36**, 703-741 (1992).
- Hunter, J. K. and M. Slemrod, "Viscoelastic fluid flow exhibiting hysteretic phase changes," *Phys. Fluids* **26**, 2345-2351 (1983).
- Larson, R. G., "Instabilities in viscoelastic flow," *Rheol. Acta* **31**, 213-263 (1992).
- Lienard, A., "Etude des Oscillations Entretenues," *Rev. Gén. de l'Electr.* **23**, 901-946 (1928).
- Lin, Y.-H., "Explanation for slip-stick melt fracture in terms of molecular dynamics in polymer melts," *J. Rheol.* **29**, 605-637 (1985).
- McLeisch, T. C. B., and R. C. Ball, "A molecular approach to the spurt effect in polymer melt flow," *J. Polym. Sci.* **24**, 1735-1745 (1986).
- Moon, F. C., *Chaotic Vibrations* (Wiley, New York, 1987).
- Petrie, C. J. S. and M. M. Denn, "Instabilities in polymer processing," *AIChE J.* **22**, 209-236 (1976).
- Sornberger, G., J. C. Quantin, R. Fajolle, B. Vergnes, and J. F. Agassant, "Experimental study of the sharkskin defect in linear low density polyethylene," *J. Non-Newt. Fluid Mech.* **23**, 123-135 (1987).
- Tordella, J. P., "Melt fracture—extrudate roughness in plastics extrusion," *SPE J.*, 36-40 (Feb. 1956).
- Uhland, E., "Das anomale Fließverhalten von Polyäthylen hoher Dichte," *Rheol. Acta* **18**, 1-24 (1979).
- Van der Pol, B., "On relaxation oscillations," *Philos. Mag.* **2**, 978-992 (1926).
- Waddon, A. J. and A. Keller, "The temperature window of minimum flow resistance in melt flow of polyethylene. Further studies on the effect of strain rate and branching," *J. Polym. Sci. (B)* **30**, 923-929 (1992).
- Weill, A., "Capillary flow of linear polyethylene melt: Sudden increase of flow rate," *J. Non-Newt. Fluid Mech.* **7**, 303-314 (1980a).
- Weill, A., "About the origin of sharkskin," *Rheol. Acta* **19**, 623-632 (1980b).
- Willems, J. H., *Stability Theory of Dynamical Systems* (Nelson, London, 1970).